Acta of Bioengineering and Biomechanics
Vol. 13, No. 4, 2011

Original paper

Mathematical study on the guidance of the tibiofemoral joint as theoretical background for total knee replacements

CHRISTOPH FIEDLER[1, 7], RICCARDO GEZZI[1, 2], KARL-HEINZ FROSCH[3], MARTIN MICHAEL WACHOWSKI[1, 4], DIETMAR KUBEIN-MEESENBURG[1, 2], JOCHEN DÖRNER[5], JOCHEN FANGHÄNEL[1, 6], HANS NÄGERL[1, 2]*

[1] Joint Biomechanical Working Group, Göttingen, Regensburg, Germany.
[2] Department of Orthodontics, Georg-August-University, Göttingen, Germany.
[3] Department of Trauma and Reconstructive Surgery, Asklepios Clinic St. Georg, Hamburg, Germany.
[4] Department of Trauma Surgery, Plastic and Reconstructive Surgery, Georg-August University Göttingen, Germany.
[5] Department of Orthopaedic & Trauma Surgery, Orthopaedicum & Parkklinik am Hainberg Northeim – Göttingen, Germany.
[6] Department of Orthodontics, University of Regensburg, Germany.
[7] ÆQUOS Endoprothetik, Munich, Germany.

The mathematical approach presented allows main features of kinematics and force transfer in the loaded natural tibiofemoral joint (TFJ) or in loaded knee endoprostheses with asymmetric condyles to be deduced from the spatial curvature morphology of the articulating surfaces. The mathematical considerations provide the theoretical background for the development of total knee replacements (TKR) which closely reproduce biomechanical features of the natural TFJ.

The model demonstrates that in flexion/extension such kinematic features as centrodes or slip ratios can be implemented in distinct curvature designs of the contact trajectories in such a way that they conform to the kinematics of the natural TFJ in close approximation. Especially the natural roll back in the stance phase during gait can be reproduced.

Any external compressive force system, applied to the TFJ or the TKR, produces two joint reaction forces which – when applying screw theory – represent a force wrench. It consists of a force featuring a distinct spatial location of its line and a torque parallel to it. The dependence of the geometrical configuration of the force wrench on flexion angle, lateral/medial distribution of the joint forces, and design of the slopes of the tuberculum intercondylare is calculated.

The mathematical considerations give strong hints about TKR design and show how main biomechanical features of the natural TFJ can be reproduced.

Key words: *tibiofemoral joint, design of TKR, instantaneous rotational axis, slip ratio, joint force distribution, force wrench, four-bar linkage*

1. Introduction

The tibiofemoral joint (TFJ) is said to be one of the most complex human articulations [1], whose biomechanical functioning is intensely debated until today. The relative motion of femur and tibia was described as combined rolling and sliding by WEBER and WEBER [2] for the first time in 1836. In 1907, FISCHER [3] specified that during knee flexion the articulating surfaces initially roll and afterwards, as soon as flexion exceeds 20–30 deg, slippage of the femur prevails. The contact areas are now practically stationary on both sides of the tibia. According to FISCHER, this kinematics is reflected in the unique migration of the instantaneous rotational axis (IRA): in knee extension, IRA-position is initially close to the contacts of the articulating surfaces and after 30 deg flexion it approaches the centers of the femoral condyles. For the first time ZUPPINGER [4] studied in vivo

* Corresponding author: Hans Nägerl, Abt. Kieferortopädie der Universität Göttingen, Klinikum, Robert-Koch-Str. 40, D-37037, Göttingen, Germany. E-mail: hnaeger1@gwdg.de
Received: February 20th, 2011
Accepted for publication: November 7th, 2011

knee movements by X-ray series. He concluded for the unloaded knee that in flexion out of full extension the femur would roll back on the tibia medially up to 12-deg flexion and laterally up to 25-deg flexion. In this regard, he suggested that the cruciate ligaments would guide the knee movement as a rigid gear unit. In 1917, STRASSER [5] definitively showed that the suggestion of Zuppinger was generally invalid and that the cruciate ligaments cannot represent the main guiding system for knee motion. Nevertheless, HUSON [6], [7] and MENSCHIK [8], [9] traced the guidance of knee motion back to that of a four-bar chain mechanism with constraint whereupon the cruciate ligaments would play the role of bars. But cruciate ligaments are not stiff rods and do not transfer compressive forces during standing or squatting. Compressive forces can only be transferred by rigid anatomical structures, i.e., the articulating surfaces [10], [11]. Hence, for knee motion under load, the force transferring structures, given by the articulating surfaces under force closure, must act as the dominant guiding system [12]. In this regard, the cruciate ligaments are a pronounced part of the perception apparatus for the instantaneous spatial knee position [12], consisting of the cruciate and collateral ligaments plus the suspensions of the menisci [13]. But, as long as the knee is unloaded, the ligaments also take over a kinematic task: they hold the femoral and tibial articulating surfaces in physiologically usable ranges of spatial set-ups. These physiological configurations of the femoral and tibial articulating surfaces are necessary in order that the articulating surfaces can immediately take over the physiological guidance when the joint is suddenly loaded with compressive forces as it is in the stance phase during gait.

For this case (the articulating surfaces are under force closure), we present theoretical considerations in the following which mathematically relate the shapes of the articulating surfaces to TFJ kinematics and TFJ force transfer for flexion/extension. Basic biomechanical point of view is: the entire set of all imaginable relative positions of tibia and femur is determined by the anatomically preset curvature morphology of the articulating surfaces. The set can be calculated once the geometric data of the articulating surfaces are known. The small cartilage deformations (<0.1 mm) under load are neglected because they do not measurably influence the relative tibia/femur positions which was stated by FISCHER [3] as early as in 1907.

For every position, tibia and femur are in contact in a medial and a lateral contact spot. Hence, two joint forces interact between femur and tibia. Neglecting friction, each force line complies with the common surface normal of the femoral and tibial articulating surface in each contact spot. Generally both force lines do not intersect. Hence in each TFJ position, the force systems transferred by the TFJ can be described by force wrenches [15]–[17]. Their geometrical structure is definitively characterized by the two surface normals and the distribution relation of the two joint forces. In each TFJ position, the possible distribution relations determine the subset of possible force wrenches.

In order to calculate successive TFJ positions, it is advantageous to limit TFJ motion to special types of movement. At first only plane movements parallel to the main functional plane of flexion/extension are considered. It is shown how kinematic features like both centrodes and the slip ratio [14] depend on the curvature morphology of the articulating surfaces and the flexional/extensional angle. Later on the mathematical scheme is to upgrade to other parameterized spatial movements.

At best, plane TFJ movements in flexion/extension are related to plane trajectories of contact on the tibial or femoral articulating surface laterally and medially. By that the articular guidance must enforce positive joint motions in flexion/extension: the articulating surfaces provide a positive cam mechanism. These notions are supported by the in vivo and in vitro MRT-measurements of TFJ motion carried out by the Freeman group [18]–[20] and the re-analyses of these works [21] as well as by measurements of posterior migration of the load bearing areas by WALKER and HAJEK [22], and by theoretical calculations made by WISMANS et al. [23]. The kinematics of this positive cam mechanism matches with the constrained kinematics of a four-bar linkage as long as the contact trajectories can be replaced by circles [12]. Then the four-bar linkage is geometrically defined by the centers of curvature of the two tibial and two femoral trajectories of contact at the articulating surfaces. The lengths of the four bars are determined by the radii of curvature of the trajectories and the positions of the centers of curvature (figures 1 and 2).

At this level of consideration outward rotations are neglected. This is initially justifiable since they seem to be too small [13] to influence the contact trajectories significantly. The influence of the ligaments is also disregarded because the ligamentous forces produced by the tensed parts of the ligaments are small in comparison to the compressing forces during the stance phase of gait. The friction forces between the femur and the tibia during gait are neglected, for these forces are small compared to the applied forces.

The aim of the following considerations is to construct a mathematical model for the TFJ under

load to deduce the example of biomechanical properties of the TFJ from geometric parameters of the articulating surfaces. The properties are as follows: a) kinematic features of TFJ motion like the centrodes or the slip ratios of the contacting articulating surfaces [14], b) geometrical configurations of forces and moments acting on the joint and c) the resulting force wrenches [15]–[17]. The mathematical model presented can be seen as the theoretical justification behind the realization of a total knee replacement (TKR) to match the kinematical properties of the natural knee, particularly during the gait cycle. The Æquos G1 [25]–[27] is the TKR constructed according to the provided theoretical scheme. Note: for the calculated relations (e.g., slip ratio and force wrench of the joint forces as the function of the flexional angle) presented in this paper, design parameters of the Æquos G1 TKR were used.

The development of the mathematical model and respective calculations are organized as follows:

Sec. 2: Flexion/extension of the TFJ is described in terms of a four-bar linkage whose geometrical parameters are derived from the curvature morphology of the trajectories of the contacts. In particular, the relations of the internal angles of the four-bar linkage are derived as functions of the flexion angle. These analytical expressions are the base for further calculations.

Sec. 3: Main kinematic relations, the centrodes and the slip ratio, are calculated depending on the flexion angle.

Sec. 4: Main features of the force transfer over the articulating surfaces are calculated as function of flexion. Since the lines of the reaction forces in the contacts of the lateral and the medial compartments do normally not intersect, the two joint forces create a force wrench whose torque depends on flexion angle, distribution of joint forces, and the slopes of the tubercula condylaria. Additionally the dependence of the torque of the wrench on geometrical parameters of the articular surfaces is calculated.

2. Methods and results

2.1. Tibiofemoral joint as four-bar linkage

Figure 1 illustrates the sagittal curvature morphology of a natural TFJ and qualitatively shows the two pairs of sagittal trajectories of contact in lateral view. Hence, femur and tibia contacting twice represent a positive cam mechanism. For the natural knee the trajectories are circularly shaped in close approximation [28], [18]–[20]. According to HAIN [29] such a positive cam mechanism is kinematically equivalent to that of a positive four-bar linkage as demonstrated in the following: the circular trajectories c_{FL} and c_{TL} in the lateral compartment are in contact at the point K_l. Their respective centers of curvature, M_{FL} and M_{TL}, lie on the common normal. The distance $M_{FL}M_{TL} = l = r_{FL} + r_{TL}$ is independent of the rotation of the femur around the pivots M_{FL} or/and M_{TL} in reference to the tibia (r_{FL}, r_{TL} = curvature radii of the trajectories at contact K_L). The guidance of the lateral compartment is characterized by the two pivots M_{FL} and M_{TL} (whose distance is l) and, in terms of kinematics, represents a dimeric link chain [10], [11]. Since in the natural TFJ both trajectories c_{FL} and c_{TL} are convexly curved [12] the position of the associated chain link l is in an *unstable* mechanical equilibrium under a compressive force acting along line l. Analogously, the circular trajectories c_{FM} and c_{TM} in the medial compartment with contacting point K_M define the medial dimeric link chain. The femur can simultaneously rotate about two curvature centers (M_{FM} and M_{FL}) at a constant distance m ($= r_{TM} - r_{FM}$) in relation to the tibia. The two pivots M_{FM} and M_{TL} again constitute a dimeric link chain. Since the convex femoral trajectory c_{FM} is now in contact with a concave curve (c_{TM}), the chain link m is mechanically *stable* under a compressive force acting along line m. Altogether the two anatomically defined dimeric link chains are linked up: since the centers M_{FM} and M_{FL} belong to the femur, bar $f = M_{FM}M_{FL}$ is fixed to the femur and specifies femur position. Correspondingly, bar $t = M_{TM}M_{TL}$ stringently defines the position of the tibia.

Result: the four centers of curvature (M_{FM} and M_{TM} together with M_{FL} and M_{TL}) form a positive four-bar linkage (figure 2) modelling TFJ motion in flexion/extension by means of a unique kinematic degree of freedom, the flexion angle φ.

Note: 1. The lengths of the four bars are independent of flexion/extension as long as the trajectories can be approximated by circles. This is true within a wide range [12], [18]. 2. The femoral medial pivot M_{FM} does not comply with the lateral one M_{FL}, because M_{FM} is anteriorly shifted with respect to M_{FL}.

The angle ε between f and t (figure 2b) corresponds to the flexion angle, $\varphi = \varepsilon_0 - \varepsilon$, where ε_0 is the value in full extension. For describing joint kinematics, the internal angles α, β, γ and δ of the four-bar linkage

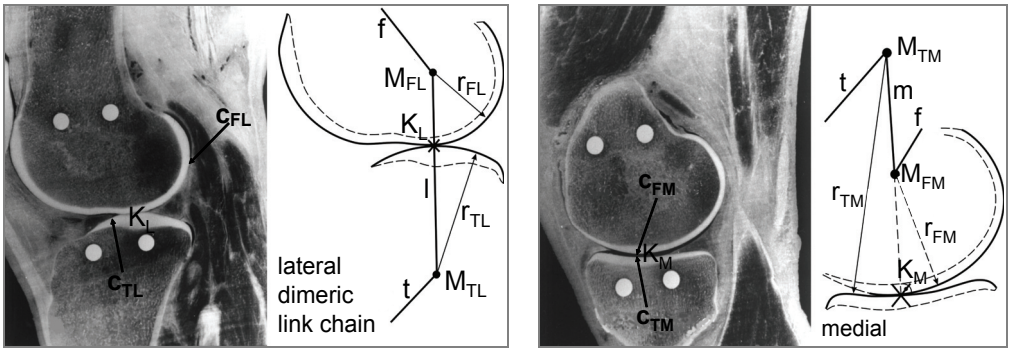

Fig. 1. Sagittal sections through a natural TFJ. Left: section through the lateral condyles reveals that the guidance by the articulating surfaces can be mapped onto an unstable dimeric link chain. Right: section through the medial condyle: the articular guidance represents a stable dimeric link chain. Further details are given in the text. White spots: fixing rods of the specimen to enable several parallel sagittal saw-cuts

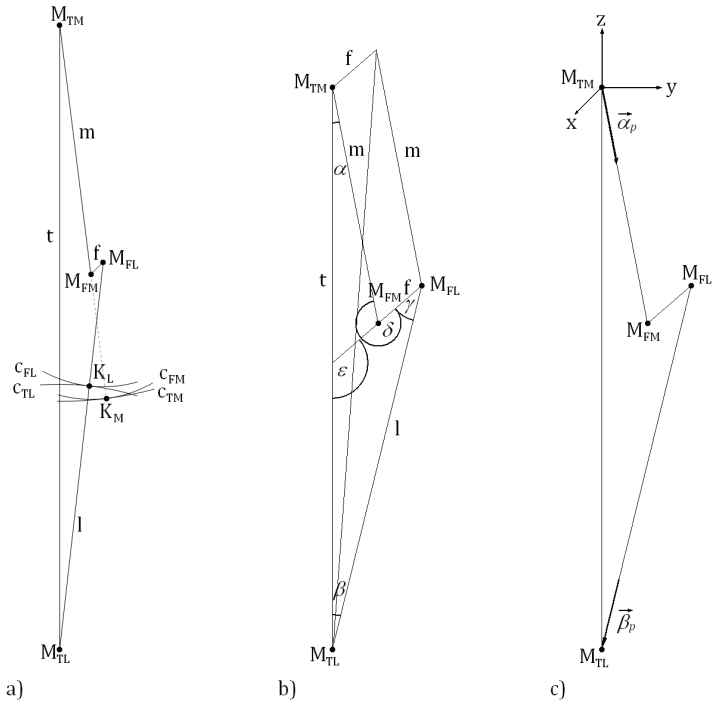

Fig. 2. Model of TFJ cam mechanism in extension: a) the two dimeric link chains (figure 1) are connected to a positive four-bar linkage with articular contact points in sagittal plane projection, b) definition of the internal angles of the four-bar linkage, c) used coordinate system: the plane of the four-bar linkage tally with the *y*–*z*-plane, the middle–sagittal plane of the TFJ

must be known as the functions of angle ε. To derive the respective functions auxiliary lines parallel to m and f were used. Thanks to the triangle, determined by t, f and ε, the internal angles can be related to angle ε, using the cosine law of plane geometry.

It holds:

$$\alpha = \varepsilon + \pi + \arccos\left(\frac{f - t\cos\varepsilon}{\sqrt{t^2 + f^2 - 2tf\cos\varepsilon}}\right) + \arccos\left(\frac{m^2 + t^2 + f^2 - l^2 - 2ft\cos\varepsilon}{2m\sqrt{t^2 + f^2 - 2tf\cos\varepsilon}}\right), \quad (1)$$

$$\beta = \arccos\left(\frac{t - f\cos\varepsilon}{\sqrt{t^2 + f^2 - 2tf\cos\varepsilon}}\right) + \arccos\left(\frac{l^2 + t^2 + f^2 - m^2 - 2ft\cos\varepsilon}{2l\sqrt{t^2 + f^2 - 2tf\cos\varepsilon}}\right), \quad (2)$$

$$\gamma = \pi - \varepsilon - \arccos\left(\frac{t - f\cos\varepsilon}{\sqrt{t^2 + f^2 - 2tf\cos\varepsilon}}\right) - \arccos\left(\frac{m^2 + t^2 + f^2 - l^2 - 2ft\cos\varepsilon}{2m\sqrt{t^2 + f^2 - 2tf\cos\varepsilon}}\right), \quad (3)$$

$$\delta = 2\pi - \arccos\left(\frac{f - t\cos\varepsilon}{\sqrt{t^2 + f^2 - 2tf\cos\varepsilon}}\right) - \arccos\left(\frac{m^2 + t^2 + f^2 - l^2 - 2ft\cos\varepsilon}{2m\sqrt{t^2 + f^2 - 2tf\cos\varepsilon}}\right). \quad (4)$$

These formulas are the basic elements of the present mathematical model of TFJ function. Equations (1)–(4) are used to calculate: a) the position of instantaneous rotational axis (IRA), b) the instantaneous slip ratio and c) the attributed geometrical relations of the force wrench transferred by the joint as the function of flexion angle $\varphi = \varepsilon_0 - \varepsilon$.

For calculating relations (1)–(4), a proper coordinate system must be defined. Advantageously the tibia should be used as reference and its line t as the z-axis pointing cranially. y-axis points posteriorly and lies parallel to the planes of the trajectories in the central sagittal plane where the origin of the coordinate coincides with the intersection point of pivot M_{TM}. Thus, y–z-plane complies with the main functional plane: the trajectories of all points of the femur run in sagittally oriented planes. When the x-axis points from the medial to the lateral side a left knee is considered (figure 2c).

For the description of the directions and positions of the force and torque vectors, it is useful to introduce auxiliary unit vectors, being collinear to the lines m and l in the y–z plane:

$$\vec{\alpha}_p = \begin{pmatrix} 0 \\ \sin\alpha \\ -\cos\alpha \end{pmatrix}, \quad \vec{\beta}_p = \begin{pmatrix} 0 \\ -\sin\beta \\ -\cos\beta \end{pmatrix}. \quad (5)$$

These vectors are determined by the internal angles α and β (figure 2b, c) and perpendicular to the contact trajectories in their corresponding contact points K_m and K_l. Further these vectors describe the force direction projected in the sagittal plane since the force can only be transferred perpendicularly to the trajectories under neglected friction.

2.2. Kinematics

2.2.1. Location of the instantaneous rotational axis

The line of a dimeric chain represents the geometric locus of intersections of all possible rotational axes of the moved body [29], [30]. Thus in the four-bar linkage, the intersection of the lines m and l of two dimeric chains definitely defines the location of IRA (figure 3a) [10], [29]. The position of the IRA can be calculated by means of triangle M_{TM} – IRA – M_{TL} using the sine law of plane geometry:

$$m_{IRA} = \frac{\sin\beta}{\sin(\alpha + \beta)} t\,. \quad (6)$$

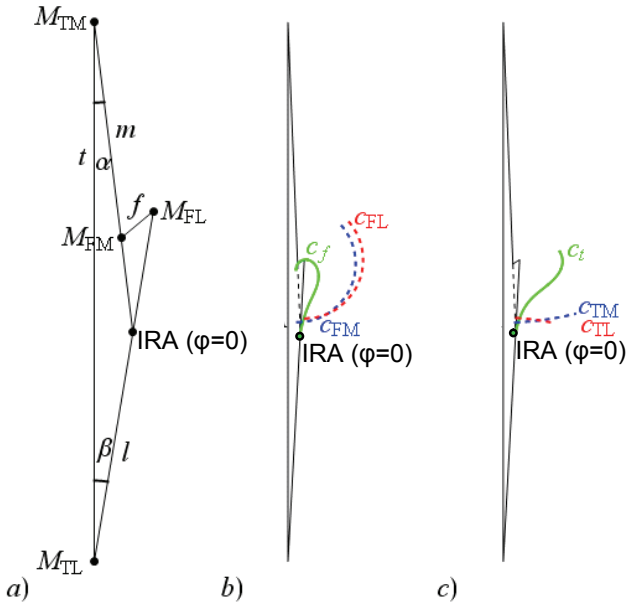

Fig. 3. a) Four-bar linkage in extension. The instantaneous rotational axis (IRA) is given by the intersection of the pivot arms m and l, b) centrode c_f fixed on the femur, c) centrode c_t fixed on the tibia
Both centrodes describe the migration of the IRA during increasing flexion. When the centrodes intersect the contact trajectories the femur is rolling on the tibia and vice versa. In extension ($\varphi = 0$) IRA lies close to the tibial or femoral articular contact curves: high percentage of rolling

Then, the coordinates $(\vec{A}_p)$ of the IRA can be specified in the sagittal plane using the unit vector of the force line $\vec{\alpha}_p$ (equation (5))

$$\vec{A}_p = m_{IRA}\vec{\alpha}_p\,. \quad (7)$$

Figures 3b and c show the two centrodes of IRA: c_t – the centrode fixed on the tibia (reference) and c_f – the centrode fixed on the femur (moving system) with the flexion angle φ as parameter. Each centrode is related to the respective body by means of the respective contact curves. The four-bar linkage is shown in full extension. Initially, the IRA is in a distal position migrates for small flexion angles near the contacts and reaches the centers of the femoral condyle for large flexion angle. At flexion angle φ = 109 deg the femur rotates about axis M_{FL}, and at φ = 134 deg about axis M_{FM}.

2.2.2. Slip ratio

For plane relative movements of two contacting bodies the slip ratio ρ is generally defined by the ratio of the velocities with which the contacts migrate on the respective articulating surfaces. Hence, the TFJ is characterized by two slip ratios, medially by ρ_m and laterally by ρ_l. They have to be calculated as the function of the flexion angle φ. To this end, the migration paths of the contact points on the articulating surfaces are written in terms of the corresponding arc lengths:

$$c_{FL} = r_{FL}(\gamma - \gamma_0), \tag{8}$$

$$c_{FM} = r_{FM}(\delta - \delta_0), \tag{9}$$

$$c_{TL} = r_{TL}(\beta - \beta_0), \tag{10}$$

$$c_{TM} = r_{TM}(\alpha - \alpha_0). \tag{11}$$

α_0, β_0, γ_0, δ_0 are the angles pertaining to the initial position of the joint. The rods of the four-bar linkage are related to the radii of the contact trajectories: $m = r_{TM} - r_{FM}$ and $l = r_{TL} + r_{FL}$ (figure 2). Using the definition of slip ratio and applying the chain rule it holds laterally or medially:

$$\rho_l = \frac{\delta_{TL}}{\delta_{FL}} = \frac{dc_{TL}/d\varphi}{dc_{FL}/d\varphi}, \tag{12}$$

$$\rho_m = \frac{dc_{TM}/d\varphi}{dc_{FM}/d\varphi}. \tag{13}$$

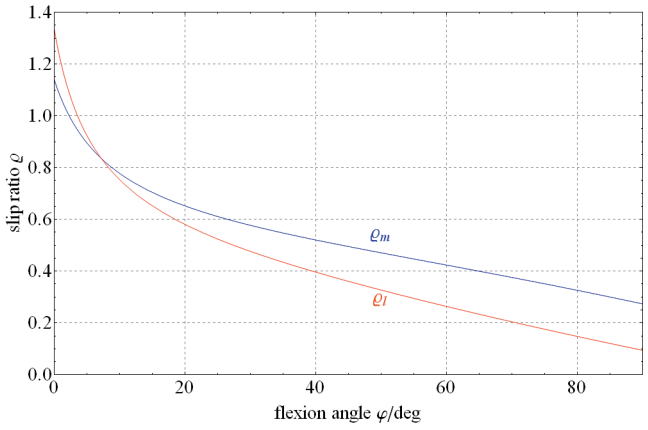

Fig. 4. Slip ratios ρ_m (medial) and ρ_l (lateral) calculated for the ÆQUOS G1 arthroplasty. For further details see text

If $\rho_{l/m} = 1$, the velocities of the contacts are identical on both respective articulating surfaces and pure rolling occurs. If $\rho_{l/m} = 0$ (∞), the contact at the tibial (femoral) surface does not move producing stationary femoral (tibial) sliding. The slip ratios ρ_m and ρ_l greatly depend on flexion angle φ (figure 4): during the stance phase, within the small flexion interval; i.e., $0 < \varphi < 25$ deg, when the knee is extremely loaded, the articulating surfaces are mainly rolling. But in the swing phase, i.e., $\varphi > 25$ deg, under low load the contacts become ever more stationary on the tibia. Therefore, the friction mechanism turns from rolling (high loaded phase) to sliding (low loaded phase).

2.3. Joint force systems

The muscular force system, which acts over the TFJ, consists of more than ten muscles. In the static case or in the stance phase of gait, this force system together with further external forces (e.g., body weight, etc.) loads the joint compressively. It must be compensated by the joint force system which consists of a medial component and a lateral one. The two force lines meet the respective centers of contact at the articular surfaces and generally do not intersect. The geometric configuration of the joint force system depends on flexion angle φ. For its calculation and clear characterization screw theory [15]–[17] is used: the force system is converted into the equivalent force wrench consisting of the resulting force possessing the definite location of the force line and the parallel torque. Note: considering the joint force system as a force wrench helps to easily and clearly describe its dependence on flexion angle, distribution of the joint forces, and dimensions of the articulating surfaces.

2.3.1. Positions of the lateral and medial joint forces

The medial and the lateral components $(\vec{F}_m, \vec{F}_l)$ of the joint force are perpendicular to the contact trajectories on the joint surfaces in the contact centers, since friction is disregarded. Hence, the lines of the joint forces coincide with the lines of the bars, m and l, in projections onto the y–z plane. In this plane, these lines are determined by angles α and β and thus by the respective unit vectors, $\vec{\alpha}_p$ and $\vec{\beta}_p$ (figure 2c, equation (5)). The unit vectors

$$\vec{\alpha} = \vec{F}_m / f_m \quad \text{and} \quad \vec{\beta} = \vec{F}_l / f_l \tag{14}$$

of the two joint forces, however, tally with the unit vectors of the contact areas. Since the contact points K_m and K_l lie on the slopes of the lateral and medial tuberculum intercondylare (figure 5) and since the contacting trajectories lie in sagittal planes, the contact areas are rotated about the tangents of the trajec-

tories at contacts K_m or K_l, respectively. These slopes of the contact areas are characterized by angles λ_m and λ_l. For computing the unit vectors $\vec{\alpha}$ and $\vec{\beta}$ of both joint forces the general rotation matrix about an arbitrary vector is applied to unit vectors $\vec{\alpha}_p$ and $\vec{\beta}_p$ [30]:

$$\vec{\alpha} = \begin{pmatrix} \sin\lambda_m \\ \sin\alpha\cos\lambda_m \\ -\cos\alpha\cos\lambda_m \end{pmatrix}, \quad \vec{\beta} = \begin{pmatrix} \sin\lambda_l \\ \sin\beta\cos\lambda_l \\ -\cos\beta\cos\lambda_l \end{pmatrix}. \quad (15)$$

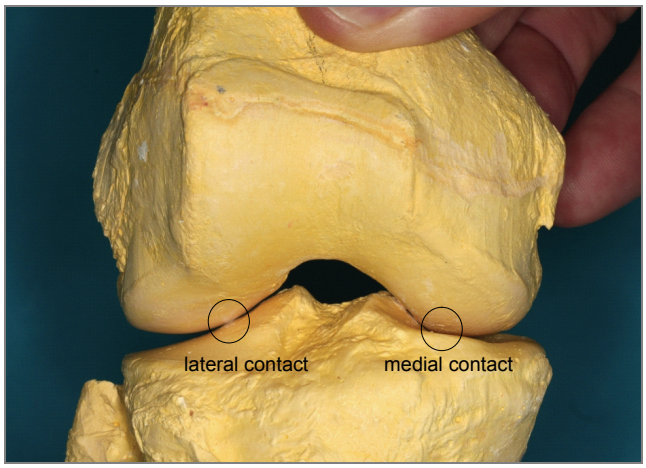

Fig. 5. True to size plaster cast of high precision of a right human TFJ with its articulating surfaces but removed menisci. Tibia and femur are arranged in extension. The lateral contact is positioned at the slope of the tuberculum condylare. The medial contact is not directly observable

Hence, the two joint forces interacting between tibia and femur are

$$\vec{F}_m = f_m\vec{\alpha} \quad \text{and} \quad \vec{F}_l = f_l\vec{\beta}\,. \quad (16)$$

As mentioned above, the respective force lines do not intersect. Therefore, the force system $(\vec{F}_m, \vec{F}_l)$ is rewritten in terms of the associated force wrench consisting of the resulting force $\vec{F}_R = \vec{F}_m + \vec{F}_l$ with an unique position of the force line and the collinear torque $\vec{T}_R$. Figure 6 illustrates the geometrical situation in 3D. The four-bar linkage is covered with the *y*–*z*-plane. The planes $M_{TM}M_{FM}$ and $M_{TL}M_{FL}$, spanned by the respective axes of the four-bar linkage, are perpendicular to *y*–*z*-plane. Thus plane $M_{TM}M_{FM}$ is necessarily parallel to the *x*-axis and contains unit vector $\vec{\alpha}_p$ and the medial contact point K_m. Therefore the common tangent $\vec{t}_m$ of both trajectories (c_{TM}, c_{FM}, figure 2a) contacting in K_m is perpendicular to this plane. Unit vector $\vec{\alpha}$ of the medial force line is rotated inwards about $\vec{t}_m$ through λ_m. Analogously, the unit vector $\vec{\beta}$ of the lateral force line is rotated through λ_l about the common tangent of trajectories (c_{TL}, c_{FL}) in contact K_l.

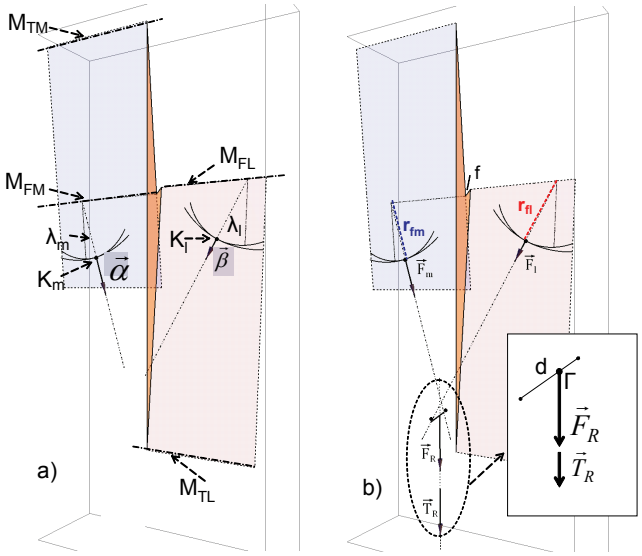

Fig. 6. 3D illustration: a) The medial and lateral condyles, respectively, are sectioned by the medial plane $M_{TM}M_{FM}$ and the lateral plane $M_{TL}M_{FL}$. The medial and the lateral planes, respectively, run through the medial (K_m) and lateral (K_l) contact points. The unit vectors $\vec{\alpha}$ and $\vec{\beta}$ are perpendicular to the respective contact area. Angles λ_m and λ_l are identical with the respective slopes of the tuberculum articulare. b) $\vec{\alpha}$ and $\vec{\beta}$ represent the unit vectors of the force lines $\vec{F}_m$ and $\vec{F}_l$. d – the shortest distance between lines $\vec{F}_m$ and $\vec{F}_l$. Γ – the intersection point of force lines $\vec{F}_R$ and d. $\vec{T}_R$ is parallel to $\vec{F}_R$. f – the distance between femoral axes M_{FM} and M_{FL}. r_{fl} – the "frontal" femoral, lateral radius produced by intersection of the $M_{TL}M_{FL}$-plane with the lateral femoral condyle. r_{fm} – the "frontal" femoral, medial radius produced by intersection of the $M_{TM}M_{FM}$-plane with the medial femoral condyle

The forces lines $\vec{l} = \vec{K}_l + \nu\vec{\beta}$ and $\vec{m} = \vec{K}_m + \nu\vec{\alpha}$ have a shortest distance, called d. The line of the resulting force $\vec{F}_R$ must intersect the line d. There exists a unique intersection point Γ of the resulting force and line d (figure 6b), at which the resulting torque $\vec{T}_R$ of the both joint forces is collinear with the resulting force $\vec{F}_R$ constituting the geometric configuration of the force wrench. Torque $\vec{T}_R$ of this force wrench is a matter of particular interest for it depends on the differing migrations of the lateral and medial contacts on the tibia and the outward slopes of the contact areas.

2.4. The force wrench produced by the two joint forces

2.4.1. General calculation

To calculate the force wrench the positions of contact points K_m and K_l (see figure 6) must be described by the respective position vectors. These are fully determined by the parameters of the four-bar linkage together with the "frontal" femoral radii (r_{fm}, r_{fl}) and the distances (d_m, d_l) from their centers to the y–z-plane:

$$\vec{K}_m = \begin{pmatrix} -d_m + r_{fm}\sin\lambda_m \\ (r_{TM} - r_{fm}(1-\cos\lambda_m))\sin\alpha \\ -(r_{TM} + r_{fm}(1-\cos\lambda_m))\cos\alpha \end{pmatrix}, \quad (17)$$

$$\vec{K}_l = \begin{pmatrix} d_l - r_{fl}\sin\lambda_l \\ (r_{TL} - r_{fl}(1-\cos\lambda_l))\sin\beta \\ -t + (r_{TL} + r_{fl}(1-\cos\lambda_l))\cos\beta \end{pmatrix}. \quad (18)$$

The shortest distance between the two force lines is given by formula [31]:

$$\vec{n} = \frac{\vec{\alpha}\times\vec{\beta}}{|\vec{\alpha}\times\vec{\beta}|}. \quad (19)$$

Vector $d\cdot\vec{n}$ can be split into two components by introducing a real number λ:

$$\begin{aligned} &\vec{d} = \vec{d}_m - \vec{d}_l = d\cdot\vec{n}, \text{ whereas} \\ &\vec{d}_m = (1-\lambda)\cdot d\cdot\vec{n} \text{ and } \vec{d}_l = -\lambda\cdot d\cdot\vec{n}. \end{aligned} \quad (20)$$

The real number λ defines a point on the line d through which the line of the resulting force $\vec{F}_R$ is supposed to run. For any supposed λ-value the moments resulting from the medial $\vec{F}_m$ and lateral force $\vec{F}$ can be calculated:

$$\vec{T}_l = \vec{d}_l \times \vec{F}_l = -\lambda\cdot d\cdot\vec{n}\times\vec{F}_l, \quad (21)$$

$$\vec{T}_m = \vec{d}_m \times \vec{F}_m = -(1-\lambda)\cdot d\cdot\vec{n}\times\vec{F}_m. \quad (22)$$

Using equations (19) and (20) equations (21) and (22) can be transformed into the relations:

$$\vec{T}_l = -\frac{\lambda d f_l}{|\vec{\alpha}\times\vec{\beta}|}(\vec{\alpha}\times\vec{\beta})\times\vec{\beta}, \quad (23)$$

$$\vec{T}_m = \frac{(1-\lambda)df_m}{|\vec{\alpha}\times\vec{\beta}|}(\vec{\alpha}\times\vec{\beta})\times\vec{\alpha}. \quad (24)$$

The resulting moment $\vec{T}_R = \vec{T}_l + \vec{T}_m$ depends on the arbitrarily taken λ-value. Applying the Lagrange formula for the vector triple product to relations (23) and (24) it follows:

$$\begin{aligned} \vec{T}_l(\lambda) + \vec{T}_m(\lambda) = \frac{d}{|\vec{\alpha}\times\vec{\beta}|}\{&\vec{\alpha}[\lambda f_l - (1-\lambda)f_m(\vec{\alpha}\cdot\vec{\beta})] \\ &+ \vec{\beta}[(1-\lambda)f_m - \lambda f_l(\vec{\alpha}\cdot\vec{\beta})]\}. \end{aligned} \quad (25)$$

This resulting moment depends on the supposed position of the line of the resulting force $\vec{F}_R$. By postulating that $\vec{F}_R$ and $\vec{T}_R$ have to be collinear in a force wrench, the spatial position of the force wrench can definitely be calculated by

$$\vec{F}_R \times (\vec{T}_l + \vec{T}_m) = 0. \quad (26)$$

Equation (26) has an unique solution $\lambda = \lambda_\Gamma$. Number λ_Γ determines the position of point Γ on line d through which the specific force line of the wrench has to run. λ_Γ can be calculated by comparing the coefficients of the linearly independent vectors $\vec{\alpha}$ and $\vec{\beta}$:

$$\begin{aligned} \lambda_\Gamma &= \frac{f_m^2 + f_l f_m(\vec{\alpha}\cdot\vec{\beta})}{f_m^2 + 2f_l f_m(\vec{\alpha}\cdot\vec{\beta}) + f_l^2} \\ &= \frac{f_m^2 + f_l f_m(\vec{\alpha}\cdot\vec{\beta})}{|f_m\vec{\alpha} + f_l\vec{\beta}|^2}. \end{aligned} \quad (27)$$

By inserting λ_Γ into relation (25), $\vec{T}_R$ becomes collinear to $\vec{F}_R$:

$$\begin{aligned} \vec{T}_R &= df_l f_m |\vec{\alpha}\times\vec{\beta}| \frac{f_m\vec{\alpha} + f_l\vec{\beta}}{|f_m\vec{\alpha} + f_l\vec{\beta}|^2} \\ &= \frac{df_l f_m |\vec{\alpha}\times\vec{\beta}|}{|\vec{F}_R|^2}\vec{F}_R. \end{aligned} \quad (28)$$

Therewith the force wrench $(\vec{T}_R, \vec{F}_R)$ is definitely characterized. The torque and force of the wrench are proportional to each other. Its factor represents the length:

$$L = \frac{|\vec{T}_R|}{|\vec{F}_R|} = \frac{df_l f_m |\vec{\alpha}\times\vec{\beta}|}{|f_m\vec{\alpha} + f_l\vec{\beta}|^2}. \quad (29)$$

Introducing the distribution relation $\mu = f_m/f_l$ into formula (29), it holds:

$$L = L(\mu, \varphi) = \frac{d(\varphi) \cdot |\vec{\alpha}(\varphi) \times \vec{\beta}(\varphi)|}{\mu + \mu^{-1} + 2(\vec{\alpha}(\varphi) \cdot \vec{\beta}(\varphi))}. \quad (30)$$

Length $L = L(\mu, \varphi)$ depends on joint force distribution and flexion angle, and additionally on slopes (λ_l, λ_m) of the tuberculum condylare, see relations (15), (17), (18) and (19).

2.4.2. Torque of the force wrench and distribution of the joint forces

Considering equation (30) $L(\mu, \varphi) = 0$ for $\mu = 0$ or $\mu^{-1} = 0$. That means: when the joint is only loaded at the lateral or the medial side, the torque $\vec{T}_R$ of the force wrench disappears. $|\vec{T}_R|$ is maximal if both compartments are loaded with equal amounts of force ($\mu = 1$). The more asymmetric the distribution of force, the smaller the torque (figure 7).

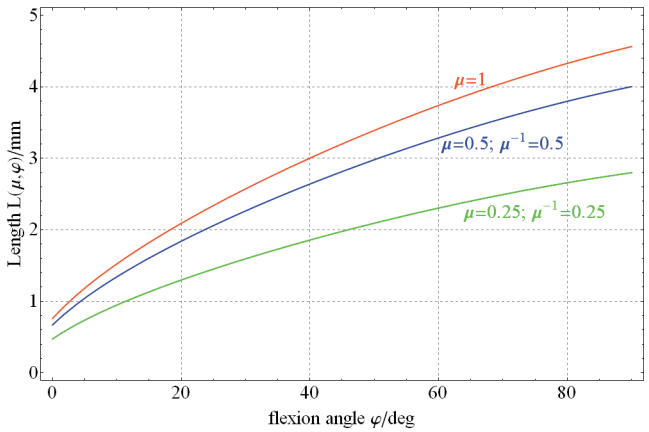

Fig. 7. $L(\mu, \varphi)$ shows a special symmetry: force distribution μ and inverse distribution μ^{-1} cause the same amount of torque. Asymmetric force distribution lowers the amount of torque

2.4.3. Location of the force wrench line and distribution of the joint forces

The location of the line of the force wrench depends on the distribution of the joint forces: equation (27) is rewritten in terms of the distribution parameter μ:

$$\lambda_\Gamma = \frac{\mu + (\vec{\alpha} \cdot \vec{\beta})}{\mu + \mu^{-1} + 2(\vec{\alpha} \cdot \vec{\beta})}. \quad (31)$$

Inserting equation (31) in equation (20), the intersection between the line of the force wrench and line d is determined:

$$\vec{d}_m = \frac{\mu^{-1} + (\vec{\alpha} \cdot \vec{\beta})}{\mu + \mu^{-1} + 2(\vec{\alpha} \cdot \vec{\beta})} d \cdot \vec{n}. \quad (32)$$

$\vec{d}_m(\mu = 1) = 0.5d \cdot \vec{n}$: the line of the resulting force meets the centre of distance d; $\vec{d}_m(\mu = 0) = 1d \cdot \vec{n}$ or $\vec{d}_m(\mu^{-1} = 0) = 0$: the force line meets the lateral or medial contact.

To calculate generally the spatial location of the force wrench line, the spatial location of line d must be determined. For this purpose, the relation between the lines of the joint forces and their minimum distance d is considered. It holds:

$$(\vec{K}_m + v_1\vec{\alpha}) - (\vec{K}_l + v_2\vec{\beta}) = d \cdot \vec{n}. \quad (33)$$

From equation (33) the real numbers v_1 and v_2 can be calculated, which define the initial and the final points of the vector $d \cdot \vec{n}$. Then, the point Γ can be found using the position vector:

$$\begin{aligned} \vec{s}_\Gamma &= (\vec{K}_l + v_2\vec{\beta}) + \lambda_\Gamma d \cdot \vec{n} \\ &= (\vec{K}_m + v_1\vec{\alpha}) - (1 - \lambda_\Gamma) d \cdot \vec{n}. \end{aligned} \quad (34)$$

Now, one point of the wrench line and its direction are given and for illustrating the force distribution on the joint, the intersection point $\vec{s}_{FR}$ with the tibia plateau can be calculated by:

$$\vec{s}_{FR}(\varphi, \mu) = \vec{s}_\Gamma + v_3 \frac{\vec{F}_R}{|\vec{F}_R|}. \quad (35)$$

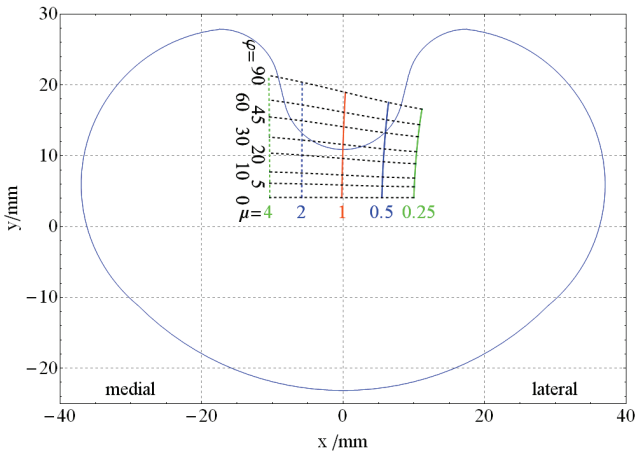

Fig. 8. Intersections of the line of the force wrench with the "tibia plateau". Both inward slopes of the tuberculum condylare (λ_m, λ_l) are assumed to be 15 deg. Parameters: a) distribution relation, $\mu = f_m/f_l$, of the joint forces; b) flexion angle φ

Figure 8 illustrates the intersections of the force lines with the tibia "plateau". The intersections migrate backwards at increasing flexion. Note: a) The migration "velocity" is high for small flexion angles indicating the initial backward rolling of the femur.

b) The position of center of load onto the interface of tibia bone/tibial part of the TKR is controlled by the distribution relation $\mu = f_m/f_l$ and the flexional angle.

2.4.4. Maximum torque and force line position of the force wrench and inward slopes of the tuberculum condylare

The maximum length L_{max} (indicating the maximum torque $\vec{T}_R$) can be significantly reduced by increasing both slopes (figure 9a) or solely the lateral slope (λ_l) (figure 9b). In the table, some remarkable values are listed for flexion angle φ = 40 deg.

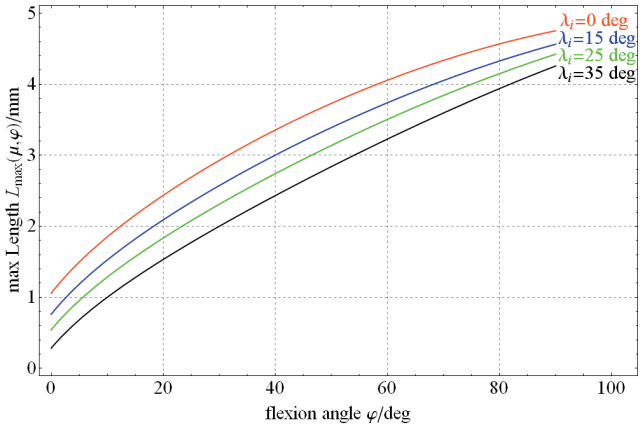

a)

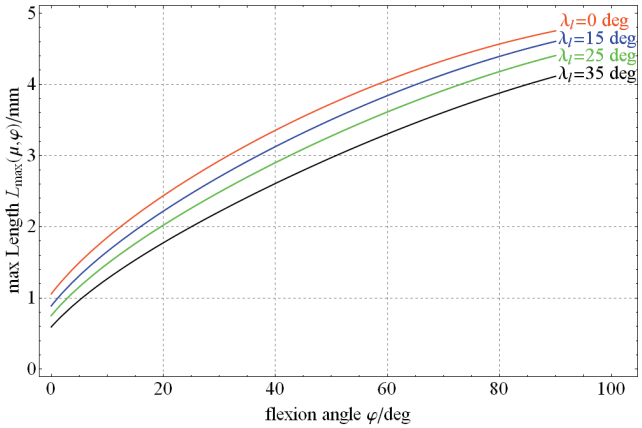

b)

Fig. 9. $L(\mu = 1) = L_{max}$ as function of flexion angle and its control by the slopes of the tuberculum condylare: a) Symmetric inward slopes of the tuberculum condylare: $\lambda_i = \lambda_l = \lambda_m$. Simultaneous increase of the slopes decreases the maximum torque of the force wrench. b) Flat medial tibia plateau: $\lambda_m = 0$. The reduction of the maximum torque can be already achieved by increasing the lateral slope of the tuberculum condylare

Table. Some aspects of reduction of axial torque of the force wrench

Medial slope λ_m (deg)	Lateral slope λ_l (deg)	L_{max} (mm) for $\mu = 1$ and $\phi = 40$ deg	Reduction of L_{max}
0	0	3.33	
15	15	3.00	10%
35	35	2.42	27%
0	35	2.60	22%

The calculation (the table, figure 9b) shows that the solely increased lateral slope takes over the main part of torque reduction: the force line is shifted to the medial side and simultaneously lowers the torque of the wrench (figure 10).

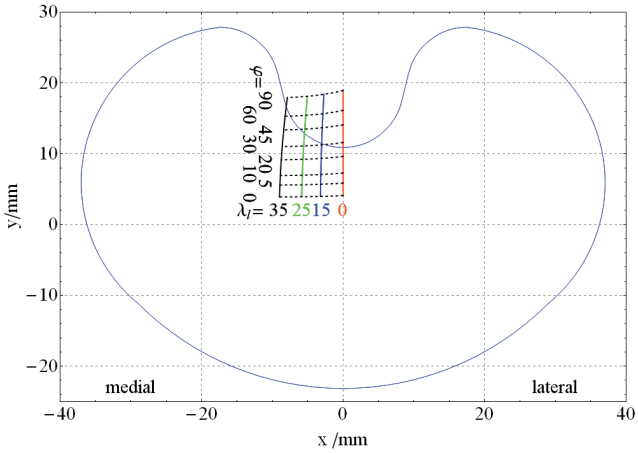

Fig. 10. Increased lateral slope of the tuberculum condylare shifts the intersections of the wrench line to the medial side of the "tibial plateau". Calculations for force distribution $\mu = \mu^{-1} = 1$

3. Discussion and conclusions

The present theoretical approach postulates that the entire set of all imaginable relative positions of tibia and femur under force closure is given by the curvature morphology of the articulating surfaces. Once the geometric data of the articulating data are known, for any preset TFJ movement the succeeding positions and with that the kinematic features and the force wrench can be calculated. It was done for plane movements in flexion/extension. The study was accomplished to achieve the aspects of the mechanics of the natural TFJ and the concepts for developing a novel type of TKR whose kinematic characteristics match as closely as possible the ones of natural knees.

Kinematics: Let us note that in flexion/extension the TFJ approximately functions like a cam mecha-

nism providing the starting point of the theoretical considerations. Following the well-known theory of gear mechanisms [29] the cam mechanism, anatomically being based upon the geometric configuration and alignment of the articulating surfaces, was replaced by an equivalent four-bar linkage. The linkage consists of four pivots, two of which, M_{TM} and M_{TL}, are fixed on the tibia and the other two, M_{FM} and M_{FL}, on the femur, whereupon M_{FM} must be anteriorly located compared to pivot M_{FL}. This morphological feature is essential to implement the particular knee kinematics: predominant rolling of the articulating surfaces out of extension and during the stance phase. Rationale: a) If the geometrically defined pivots of both femoral condyles coincided, the knee joint would imperatively constitute an unphysiological simple hinge joint with a femorally fixed rotational axis for flexion/extension, albeit the tibial contact trajectories have been opposed to sagittal curvatures. In this case, initial rolling would be definitively impossible. b) If vice versa, pivot M_{FL} would be anterior to M_{FM}, the TFJ could not be flexed but only extended. c) M_{FM} anterior to M_{FL} positioned makes that in extension the initial position of the IRA can be laid near the contacts of the cam mechanism as it is demonstrated by the respective centrodes fixed on the tibia or the femur (figure 3). The shape of femorally fixed centrode measured by FISCHER [3] more than 100 years ago appears to be close to our calculations.

The calculated slip ratio–flexional angle characteristics (figure 4) of the four-bar-chain model exemplifies how the natural knee solves the friction problem: out of extension the articulating surfaces initially roll back (range: $\varphi < \approx 25°$) and afterwards predominantly slide. Finally, in further flexion, the articulating contacts become stationary on the "tibia plateau". These slip ratios are also consistent with re-analyses by carried out NÄGERL et al. [21] of some papers of the "Freeman group" [18]–[20]. NÄGERL et al. [21] showed that under load the natural TFJ mainly rolls (≈ 90%) during the stance phase ($\varphi < \approx 25°$). The central concept defining the ÆQUOS TKR was to implement a predominant rolling of the articulating surfaces during the stance phase (figure 4) produced by the shaping of these surfaces. Rationale: by this rolling the mechanical stressing of the polyethylene inlay (which is extremely compressed in the stance phase) is minimized for the following mechanical reasons: a) shear stressing is significantly reduced, b) static friction, which would be caused by sliding friction at reversal of motion, is avoided, and c) the inlay is permanently rinsed and thus cooled by synovia. By in vivo measurements of the kinematic profile of 14 patients with ÆQUOS TKR WACHOWSKI et al. [30] have shown that this TKR is really rolling in the stance phase.

Joint force system: The force system, transferred by the natural TFJ or the ÆQUOS arthroplasty, generally represents a force wrench because at physiologic joint positions the spatial vectors of the lateral and medial joint forces do not define planes. The necessarily appearing torque must be taken into account for a better understanding of the TFJ mechanics or TKR functioning.

In anatomical or orthopedic textbooks and in papers concerning knee function, the torque of the joint forces is normally neglected. This torque can be described by a multivariable function depending on flexion angle, joint force distribution, and dimensions of the TFJ or the arthroplasty. The torque increases monotonically with increasing flexion angle. It can be minimized via joint force distribution (figure 7) by shifting the resulting force line towards the lateral or medial joint contact (figure 8) and besides controlled by the respective torque of the force wrench by the muscular system. In this regard, the uni-articular muscles, i.e., popliteus m. (internal rotation) and caput breve of the biceps femoris m., play central roles [31].

The calculations show that the shaping of the tibial articulating surfaces, as especially implemented by the degree of the slopes of the tuberculum condylare, is correlated to the amount of the torque (figures 9a,b). Simultaneously the spatial location of the line of the force wrench is laid down by these slopes (figure 10). An increase in a lateral slope loads the medial part of the tibia. In the natural knee, the slopes are really asymmetric. Laterally, the slope at the contact neighbourhood is steeper than medially and roughly amounts to 35 deg (figure 5). According to the results of the present model these asymmetric anatomical features obviously serve to effectively reduce the torque of the joint force wrench and to keep it in ranges which can be controlled by the respective axial torque produced by the muscular system acting over the TFJ, especially by the uni-articular muscles popliteus and caput breve of the biceps femoris. Note: by this anatomical asymmetry the medial part of the knee is mainly loaded (figure 10).

The present theoretical scheme is a useful tool for running and further development of knee arthroplasties with physiologic properties: by the shaping of the contact trajectories the kinematics of the TKR approaches that of the natural TFJ and by the shaping of

the slopes of the artificial tuberculum condylare the force transfer approximates to the force transfer in the natural TFJ.

The model described in its present form is limited to plane movements in flexion/extension. As already mentioned above, it can be upgraded to spherical or otherwise parameterized movements in flexion/extension so that the biomechanical properties of the TKR approach the natural TFJ still better.

According to the laws of spatial kinematics of rigid body [34], the natural TFJ and also ÆQUOS–TKR feature four kinematical degrees of freedom (DOF) because of the two contact spots. The "main" DOF, flexion/extension, which was modelled, assuming that its large excursions can be described by plane movements, is actively controlled by the muscular system. The three "small" DOFs, however, cannot be actively adjusted by the muscular system. They are ab-/adduction and two axial rotations whose corresponding axes are given by the two surface normals of the contact spots. Needless to say, these movements are possible. They can be enforced by external perturbing forces and moments in each flexional/extensional state of the TFJ. Therefore each state must be mechanically stable in relation to these "small" DOFs. That means: as soon as the "perturbation" does not act any longer on the TFJ, it must automatically return to its original state. The extent of this mechanical stability can be controlled by the muscular tonus. For flexion/extension NÄGERL et al. [12] made graphically evident that the quality of stability can be adjusted by the muscular apparatus from stability to indifference or instability and vice versa. Calculations of these important problems of mechanical stability will be presented in a future paper.

References

[1] BAUMGARTL E., *Das Kniegelenk*, Springer Verlag, Berlin 1964.

[2] WEBER W., WEBER F., *Mechanik der menschlichen Gehwerkzeuge*, Göttingen, Translated by Maquet P. and Furlong R. (1992): *Mechanics of the human walking apparatus.* Section 4: *On the knee*, Springer Verlag, Berlin, 1992.

[3] FISCHER O., *Kinematik organischer Gelenke*, Vieweg-Verlag, Braunschweig, 1907.

[4] ZUPPINGER H., *Die active Flexion im unbelasteten Kniegelenk*, Züricher Habil Schriften Bergmann Verlag, Wiesbaden, 1904.

[5] STRASSER H., *Lehrbuch der Muskel- und Gelenkmechanik.* Vol. III: Special section entitled: *Die untere Extremität*, Springer Verlag, Berlin, 1917.

[6] HUSON A., *The functional anatomy of the knee joint: the closed kinematic chain as a model of the knee joint*, Proc. Int. Congr, 1973 (334), 163.

[7] HUSON A., *Biomechanische Probleme des Kniegelenks*, Orthopädie, 1974, 3, 19.

[8] MENSCHIK A., *Mechanik des Kniegelenkes*, 1. Teil. Z. Orthop., 1974, 112, 481.

[9] MENSCHIK A., *Mechanik des Kniegelenkes*, 2. Teil *Schlußrotation*, Z. Orthop., 1975, 113, 388.

[10] KUBEIN-MEESENBURG D., NÄGERL H., COTTA H., FANGHÄHNEL J., *Biomechanische Prinzipien in Diarthrosen und Synarthosen*, Teil I. *Grundbegriffe bei Diarthrosen*, Z. Orthop., 1993, 131, 97.

[11] KUBEIN-MEESENBURG D., NÄGERL H., FANGHÄHNEL J., *Elements of a general theory of joints:* 1. *Basic kinematic and static function of diarthrosis*, Anat. Anz., 1990, 170, 301.

[12] NÄGERL H., KUBEIN-MEESENBURG D., COTTA H., FANGHÄHNEL J., *Biomechanische Prinzipien in Diarthrosen und Synarthosen*, Teil III. *Mechanik des Tibiofemoralgelenkes und Rolle der Kreuzbänder*, Z. Orthop., 1993, 131, 385.

[13] NÄGERL H., KUBEIN-MEESENBURG D., MIEHE B., FANGHÄNEL J., *The sensory apparatus for perception in the tibiofemoral joint and outlines of a functional knee endoprosthesis*, Acta of Bioengineering and Biomechanics, 2002, 4, Suppl. 1, 319.

[14] ZATSIORSKY V.M., *Kinematics of Human Motion*, Human Kinetics Publisher, Champaign, Illinois, 1998.

[15] BALL R.S., *The theory of screws: A study in the dynamics of a rigid body*, Hodges, Foster, Dublin, 1876.

[16] TIMBERDING H.E., *Geometrie der Kräfte*, Teubner, Leipzig, 1908.

[17] YANG A.T., *Calculus of screws*, [in:] *Basic Questions of Design Theory*, W.R. Spillers (editor), Elsevier, 1974, 266–281.

[18] IWAKI H., PINSKEROVA V., FREEMAN M., *Tibiofemoral movement 1: The shapes and relative movements of the femur and tibia in the unloaded cadaver knee*, The Journal of Bone and Joint Surgery (BR), 2000, 82B, 1189.

[19] PINSKEROVA V., IWAKI A., FREEMAN M., *The shapes and relative movements of the femur and tibia in the unloaded cadaveric knee: A study using MRI as an anatomical tool*, [in:] N. Insall (Hrsg.), R. Scot (Hrsg.), W.B. Saunders (Hrsg.), *Surgery of the knee*, third edition, 2001.

[20] PINSKEROVA V., JOHAL P., NAKAGAWA S., SOSNA A., WILLIAMS A., GEDROYC W., FREEMAN M., *Does the femur roll back with flexion?* The Journal of Bone and Joint Surgery, 2004, BR 86-B, 925.

[21] NÄGERL H., WALTERS J., FROSCH K.-H., DUMONT C., KUBEIN-MEESENBURG D., FANGHÄNEL J., WACHOWSKI M.M., *Knee motion analysis of the non-loaded and loaded knee: a re-look at rolling and sliding*, Journal of Physiology and Pharmacology, 2009, 60, Suppl. 8, 69.

[22] WALKER P.S., HAJEK J.V., *The load bearing area on the knee joint*, Journal of Biomechanics, 1972, Vol. 5, 581–589.

[23] WISMANS J., VELDPAUS F., JANSSEN J., HUSON A., STRUBEN P., *A three-dimensional mathematical model of the knee joint*, J. Biomechanics, 1980, 13, p. 677–85.

[24] KOH J., GRABINER D., SWART D. de, *In vivo tracking of the human patella*, J. Biomechanics, 1991, 25, p. 637.

[25] FROSCH K.-H., FLOERKEMEIER T., ABICHT C., ADAM P., DATHE H., FANGHÄNEL J., STÜRMER K.M., KUBEIN-MEESENBURG D., NÄGERL H., *Eine neuartige Knieendoprothese mit physiologischer Gelenkform*. Teil 1: *Biomechanisch Grundlagen und tribologische Untersuchungen*, Unfallchirurg., 2009a, 112, 168–175.

[26] FROSCH K.-H., NÄGERL H., KUBEIN-MEESENBURG D., DÖRNER J., DATHE H., HELLERER O., DUMONT C., STÜRMER K.M., *Eine neuartige Knieendoprothese mit physiologischer Gelenkform*.

Teil 2: *Erste klinische Ergebnisse*, Unfallchirurg., 2009b, 112, 176–184.

[27] NÄGERL H., FROSCH K.-H., WACHOWSKI M.M., DUMONT C., ABICHT C., ADAM P., KUBEIN-MEESENBURG D., *A novel total knee replacement by rolling articulatings surfaces. In vivo functional measurements and tests*, Acta Bioeng. Biomech., 2008, 10, 55.

[28] HISS E., SCHWERBOCK B., *Untersuchungen zur räumlichen Form der Femurkondylen*, Z. Orthop., 1980, 118, 396.

[29] HAIN K., *Angewandte Getriebelehre*, Hermann Schroedel Verlag K.G., Hannover, Darmstadt, 1952.

[30] WACHOWSKI M.M., FIEDLER C., WALDE T.A., BALCAREK P., SCHÜTTRUMPF J.P., FROSCH S., FROSCH K.-H., FANGHÄNEL J., GEZZI R., KUBEIN-MEESENBURG D., NÄGERL H., *Construction-conditioned rollback in total knee replacement: fluoroscopic results*, Acta Bioeng. Biomech., 2011, 13(3), 35–42.

[31] KAPANDJI I.A., *Funktionelle Anatomie der Gelenke.* Band 2: *UntereExtremität*, Ferdinand Enke Verlag, Stuttgart, 1985, 142.